Analysis of micro-lens integrated flip-chip InGaN light-emitting diodes by confocal microscopy

K. H. Li, C. Feng, and H. W. Choi

Articles you may be interested in

Enhanced light extraction efficiency in flip-chip GaN light-emitting diodes with diffuse Ag reflector on nanotextured indium-tin oxide
Appl. Phys. Lett. **93**, 021121 (2008); 10.1063/1.2953174

Single-step fabrication of Fresnel microlens array on sapphire substrate of flip-chip gallium nitride light emitting diode by focused ion beam
Appl. Phys. Lett. **91**, 051111 (2007); 10.1063/1.2757602

Mesa-size-dependent color contrast in flip-chip blue/green two-color In Ga N Ga N multi-quantum-well micro-light-emitting diodes
Appl. Phys. Lett. **89**, 093501 (2006); 10.1063/1.2339034

Optical cavity effects in InGaN/GaN quantum-well-heterostructure flip-chip light-emitting diodes
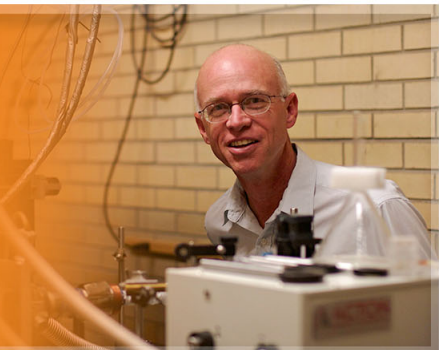Appl. Phys. Lett. **82**, 2221 (2003); 10.1063/1.1566098

High-power AlGaInN flip-chip light-emitting diodes
Appl. Phys. Lett. **78**, 3379 (2001); 10.1063/1.1374499

Analysis of micro-lens integrated flip-chip InGaN light-emitting diodes by confocal microscopy

K. H. Li, C. Feng, and H. W. Choi[a)]
Department of Electrical and Electronic Engineering, The University of Hong Kong, Hong Kong

A hexagonally close-packed microlens array has been integrated onto the sapphire face of a flip-chip bonded InGaN light-emitting diode (LED). The micro-optics is formed by etching a self-assembled monolayer of 1-μm silica microspheres coated on the sapphire substrate, producing hemispherical sapphire lenses. Without degrading electrical characteristic, the light output power of the lensed LED is increased by more than a quarter compared with the unlensed LED. Enhanced light extraction via micro-optics is verified by rigorous coupled wave analysis. The focusing behavior of the micro-lenses, as well as the emission characteristics of the lensed LED, is studied by confocal microscopy. © *2014 AIP Publishing LLC*. [http://dx.doi.org/10.1063/1.4863925]

Besides general lighting applications, III-nitride light emitting diodes (LEDs) have also been used for highly directional lighting purposes, including projectors, flashlights, automobile headlamps, and fiber-coupled light sources. Typically, external optical components, such parabolic reflectors and collimators, are required to condense the original Lambertian emission pattern into a narrower beam with reduced divergence. However, such converging processes impose various limitations, including poor optical coupling efficiencies and restricted system robustness due to bulky optical components. A more elegant approach involves the elimination of external optics through monolithic integration of lenses directly onto the chip,[1–3] this is particularly suitable for devices in the flip-chip configuration,[4,5] whereby the transparent sapphire substrate is exposed, becoming the light extraction surface. The sapphire surface is free of bond-wires, making it ideal for integration of optics, which enables modification of emission behavior, as well as enhancement of light extraction. As LED chips are typically of dimensions in the range of 300 to 1000 μm, the optical components will also have to be of micrometer scales. On top of that, devices packaged in the flip-chip configuration are capable of efficiently dissipating the generated heat to the sub-mount. Although the sapphire-air interface offers a reduced refractive index contrast compared to GaN-air, the planar surface becomes the bottleneck restricting light extraction due to total internal reflections. Techniques to texture the sapphire surface, such as dry etching[6] and wet etching combined with chip shaping processes,[7] have been demonstrated as effective means of promoting light extraction.

One of the most common ways of forming micro-optics is definition through photo-lithography followed by photoresist reflow for reshaping the disk-shaped pedestals into domes.[2,3] Due to the limited optical resolution of photolithography, gaps between lenses are inevitable, limiting the lens coverage area to around 50%–57%. Moreover, the photoresist masking layer may not be able to offer sufficient selectivity to form high aspect ratio micro-optical elements

onto hard sapphire during dry etching, resulting in insignificant H_L/D ratio of micro-lenses of 0.07–0.08, where H_L is the height at the vertex and D is the diameter of curvature. Nanosphere lithography (NSL) is adopted in this work; NSL is capable of forming large-area periodic micro- and nano-structure at minimal cost and high efficiencies, a distinct advantage over other high resolution patterning techniques such as electron beam or nano-imprint lithography. As feature dimensions correspond roughly to the diameters of the nanospheres, the NSL process is highly scalable producing periodic structures with feature sizes as small as tens of nanometers. Additionally, the use of hard nanospheres (such as silica or alumina) provides the selectivities needed for pattern transfer onto hard materials such as sapphire. Self-assembled nanosphere arrays have previously been used to form two-dimensional periodic nanostructures on the p-GaN,[8] n-GaN,[9] and sapphire[10] faces of InGaN LEDs.

In this work, a two-dimensional hexagonal closed packed (hcp) monolayer of silica spheres serves as an etch mask to form micro-lenses on the sapphire surface of flip-chip InGaN LEDs. The silica spheres provide comparable etch resistance and selectivity to sapphire enabling the formation of hemispherical lenses. The optical characteristics of the devices are compared with conventional flip-chip LEDs. Rigorous coupled wave analysis (RCWA) is performed to determine the role of the hcp lens array towards light extraction efficiency. The focusing behavior of the lenses and the emission pattern of the lens-integrated devices are evaluated by the confocal microscopy.

The epitaxial wafers consisting of InGaN/GaN quantum wells (QWs) are grown by metal-organic chemical-vapor deposition (MOCVD) on (0001) sapphire substrates. The sapphire substrate is initially lapped down to ~80 μm followed by polishing to optical smoothness. A 200 nm semi-transparent indium-tin-oxide (ITO) film serving as current-spreading layer is deposited on top of p-GaN. A mesa region of 500×200 μm^2 is defined by a photolithography and a Cl_2-based plasma is used to expose n-GaN surface. The contact regions are defined by another photolithographic step and metal pads are coated by e-beam evaporation. Metal lift-off is followed by rapid thermal annealing to form ohmic

a)Author to whom correspondence should be addressed. Electronic mail: hwchoi@hku.hk. Tel.: (852) 28592693. Fax: (852) 25598738.

contacts. Subsequently, NSL is employed to form a masking pattern on the sapphire surface. Silica spheres with mean diameters of $1\,\mu m$ are diluted in deionized water until it reaches an optimized concentration of 2% solids. Sodium dodecyl sulfate (SDS) is mixed with the colloidal suspension at a volume ratio of 1:10, in order to reduce the surface tension of the aqueous mixture. A $10\,\mu L$ droplet of the mixture is pipetted onto the sapphire surface and the spheres are dispersed into an hcp monolayer by spin-coating at 500 rpm. The pattern is transferred onto sapphire by inductively coupled plasma (ICP) etching using a gas mixture of SF_6/He. The coil and platen powers are maintained at 400 W and 100 W under a constant pressure of 5 mTorr. During the etch process, the spheres shrink in both lateral and vertical directions, forming smooth and curved sidewalls, finally becoming hemispheres upon complete removal of the particles. The wafers are diced by ultraviolet (UV) laser micro-machining, and the dies are flip-chip bonded onto a ceramic sub-mount, as illustrated in the schematic diagram shown in Fig. 1(a). Identical LEDs without the lens arrays are fabricated alongside for comparisons. The surface morphologies of the lenses are imaged using atomic force microscopy (AFM). From the AFM image shown in Fig. 1(b), the diameters and heights of the lenses are $1\,\mu m$ and $0.35\,\mu m$, respectively, corresponding to a hemispherical curvature with an H_L/D ratio of 0.35. The scanning electron microscope (SEM) image in Fig. 1(c) provides another view of the microlenses.

Fig. 2(a) shows the light-current-voltage (L-I-V) characteristics of the LEDs. It is observed that the electrical properties, including turn-on voltages and dynamic resistances, of the lensed LED are hardly different from that of the unlensed device; after all the additional lens processing is carried out on the sapphire face and would not degrade the device electrical performance. The light output powers of the un-encapsulated devices are then measured in a 12-in. integrating sphere coupled to a calibrated spectrometer (Ocean Optics HR2000) via an optical fiber. The plots of optical powers versus currents are also shown in Fig. 2(a). At a current of 90 mA, the light output power of lensed LED is roughly one quarter higher than that of the flat-top LED.
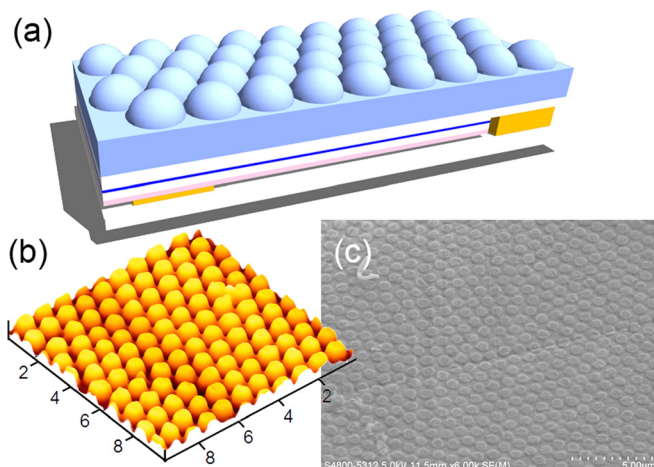

FIG. 1. (a) Schematic diagram depicting the flip-chip LED with a microlens array on the sapphire surface; (b) AFM and (c) SEM images showing the hemispherical lens array.
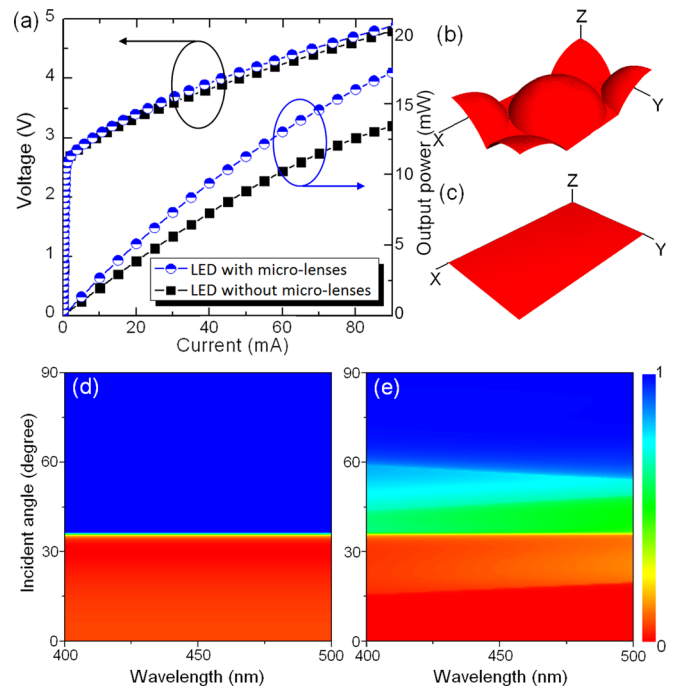

FIG. 2. (a) L-I-V characteristics of the flip-chip LEDs with and without lenses; defined unit cells of (b) periodic lens array and (c) flat-top structure for RCWA simulations; the computed reflectivities of the (d) flat-top profile and (e) lens array; the linear scale bar on the right represents reflectivities of incident light.

This shows that the microlens-integrated emitter can partially extract the guided light by reducing the amount of total internal reflections and thereby lowering the photon reabsorption losses. To investigate how the periodic lens array can reduce the internal reflections, RCWA, widely used for the analysis of scattering electromagnetic waves from periodic structure, is performed on the device structures. The calculated electromagnetic fields as a sum over coupled waves are obtained by solving Maxwell's equations in the Fourier domain. The resultant reflectivity is the sum of the reflected diffraction efficiencies of all modes. Note that the infinite periodic boundary condition is implemented in the calculation and the unit cells as shown in Figs. 2(b) and 2(c) are assumed to be extended infinitely across the x-y plane. Since the flip-chip LEDs contain QWs emitting at a center wavelength of 440 nm and full-width-at-half-maximum (FWHM) of $\sim$23 nm, the reflectivities over the wavelength range of 400–500 nm are computed to ensure that the emission band is fully covered. Not unexpectedly, a sharp contrast in reflectivity at $\sim$34.6° is observed in Fig. 2(d). When light rays strike the flat-top surface at an angle large than 34.6°, its reflectivity instantaneously rises to unity, corresponding to the critical angle at the interface between sapphire and air. It is consistent with the Snell's law, whereby the critical angle can be determined as $\sin^{-1}(n_{air}/n_{sap}) = 34.2°$, where n_{air} and n_{sap} are the refractive indexes of air and sapphire, respectively. On the other hand, the lenses significantly weaken the overall reflectivity over a range of incident angles up to $\sim$58°, thus enlarging the light-escape cone of the LED and allowing more trapped light to be extracted. Of course, the effects will be diminished upon epoxy encapsulation; nevertheless, simulation data (not presented here) indicate that the

enhancement remains significant even with encapsulation compared to a planar sapphire surface.

Apart from light extraction, the microlens arrays also play a role in altering the emission pattern of LED. Typically, the emission profile from light sources is performed by goniophotometry, whereby the angular light intensities are obtained to produce a 2-D spatially resolved radiation pattern. A constant separation distance between the detector and light source—an LED in this case—must be maintained for accuracy, since the dimension, geometry, and package of the LED can severely affect the detected signals. Therefore, goniophotometry is generally adopted for measuring far-field patterns. However, micro-lenses operate in the "mid-field" range, at micrometers to hundreds of micrometers from the optical elements (the term "near-field" being reserved for sub-wavelength distances). To provide a comprehensive view in both the mid- and far-field emission distributions, 3-D intensity mapping of the LEDs is acquired by confocal microscopy[11] (Carl Zeiss LSM700). Only light rays emanating from the focal plane can be detected by the photomultiplier tubes (PMT), while "out-of-focus" light is effectively suppressed by the diameter-adjustable pinhole. After multiple planar x-y plane confocal images are continuously captured along the z-axis, the 3-D emission model can be reconstructed by stacking the captured slices, from which cross-sectional views of the emission cone can be generated. In order to be able to capture the propagation characteristics of individual 1-μm lens elements, a high magnification 150$\times$ (N.A. = 0.95, acceptance half-angle $\theta = 72.1°$) dry objective lens is used. For this experiment, a microlens array is fabricated on an identical LED wafer, without having the device fabricated. A blue collimated laser beam (continuous wave diode-pumped solid-state laser, $\lambda = 473$ nm) is incident upon the planar GaN surface in the perpendicular direction. The detected signals are adjusted to be mildly over-exposed in order to enhance the contrast of the images. Figs. 3(a) and 3(b) show planer confocal images recorded at the device surface plane and the focal plane of the lens array; the diameters of the light spots correspond roughly to the diameters of the lenses and the focused spot size, respectively. To highlight the focusing behavior of the lenses, a cross-sectional view of the stacked confocal images is reconstructed, as illustrated in Fig. 3(c). As can be seen, all light rays are within the acceptance angle of the objective lens. The collimated beams condense into a spot at a distance of 0.670 μm from the sapphire surface. The focal length (f) of the lenses[12] can be calculated as $f = (h + r)/(2hn_{sap} - 2h) = 0.682\ \mu$m, where h and r are the radius and height of lenses, respectively. The calculated value is in good agreement with the value measured by confocal microscopy. Fig. 3(d) shows a comprehensive 3-D view of the combined focal images, illustrating focusing of the collimated laser beam into distinct light cones by the micro-lenses.

Although an objective lens with a lower magnification increases the field of view (FOV) to capture the emission from an entire chip, its lower numerical aperture (N.A.) also restricts its ability to collect light at wider angles.[13] To ensure that light emission from the devices at all angles is sufficiently detected, the signals are collected with a 50$\times$ dry objective (N.A. = 0.8, $\theta = 53.2°$). To overcome the limited
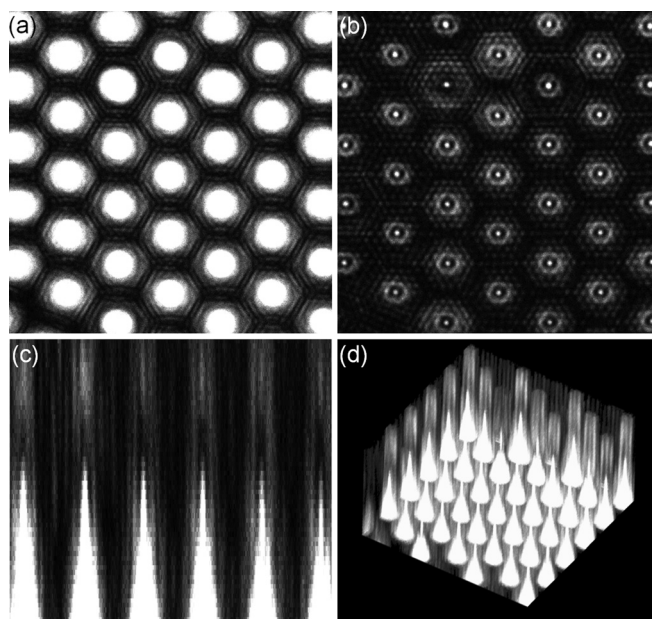

FIG. 3. Confocal images with a capture area of $5.11 \times 5.11\ \mu m^2$ along the x-y plane captured at (a) the sapphire surface and (b) the focal plane of the lenses; (c) cross-sectional view ($5.11 \times 1.09\ \mu m^2$ along x-z plane) of the stacked confocal slices; (d) three-dimensional view of the combined confocal images illustrating the light cones modified with the micro-lenses.

FOV, a tile-based scanning algorithm is applied to obtain a stitched area of $115\ \mu$m $\times\ 1017\ \mu$m. Nine confocal plane images were captured over a z-distance of 600 μm. Figs. 4(a) and 4(b) illustrate cross-sectional views of light intensity distributions of the unlensed and lensed LEDs operated at 80 mA. As observed, all non-zero data points fall within the acceptance cone of the objective, justifying the use of the
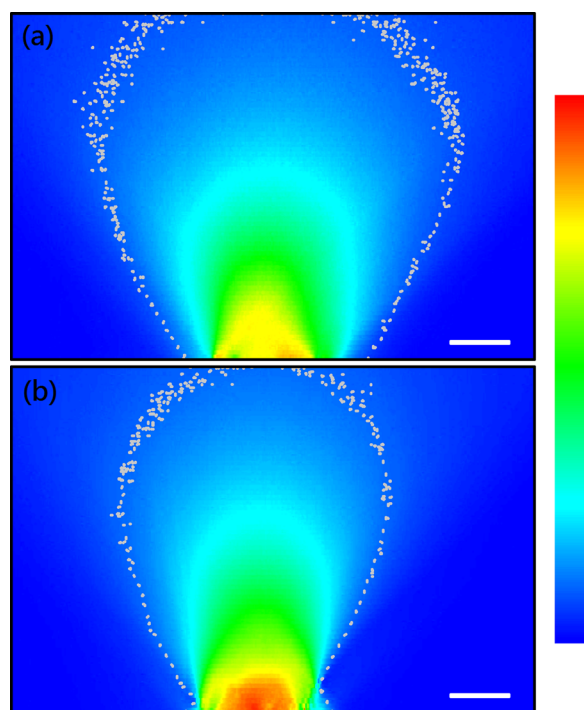

FIG. 4. Confocal emission patterns of (a) unlensed and (b) lensed LEDs. The scale bar represents the emission light intensity (red: maximum value, blue: minimum value). The grey dotted lines represent the 10% angular intensity point, while the white scale bar corresponds to 120 μm.

$50\times$ objective. It can be seen that the light intensities of the lensed LED are significantly higher particularly in the vicinity of the chip; this observation is consistent with simulated results and L-I measurements in earlier discussions. Additionally, the lensed LED emits with reduced divergence compared with the unlensed LED, due to the focusing abilities of the microlenses. While the cross-sectional emission plots provide direct visual information on the light spatial distribution, a systematic analytical method needs to be adopted for quantitative comparisons. The annotated dotted lines in Figs. 4(a) and 4(b) represent an angular plot, whereby the optical intensities have dropped to 1/10 of their maximum intensities at that particular angle. Quantitatively, the maximum width of the dotted line (the 10% intensity boundary) is reduced by one-third compared with unlensed LED.

It would be also interesting to devise a relation between data generated from confocal microscopy and goniophotometry for comparisons. One-dimensional (1-D) angular plots can be obtained from the two-dimensional (2-D) cross-sectional confocal microscopy data by setting the position of the LED as the origin, and extracting the light intensity data points at a fixed radius away from the origin at regular angular intervals, with the aid of Matlab. Normalized angular plots generated this way for the LEDs with and without micro-lenses are plotted in Fig. 5(c). The radius and angular resolution are $\sim$230 μm and 0.5°, respectively; plots generated at other distances (not shown) have been found to yield similar profiles. The FWHM emission divergence angles are evaluated as 83.7° and 61.0° for the unlensed and lensed devices, respectively, corresponding to a reduction of divergence by $\sim$27%. Normalized goniometric angular plots, measured at a distance of 50 mm from the devices, are also plotted in Fig. 5(c). The FWHM angles for the unlensed and lensed LEDs are 132.1° and 113.1°, respectively,

corresponding to a decrease of $\sim$14%. An appreciable amount of generated light is trapped within the planar sapphire substrate,[14] which propagates in the form of guided modes and tends to escape through the facet of the device, thus broadening the emission. The micro-lens array is capable of re-directing laterally propagating photons into the vertical direction to reduce emission from the facets, thus contributing to the reduced divergence.

The discrepancies between data obtained from confocal microscopy and goniophotometry can be explained in terms of the differences in the way light is collected, as depicted in the schematic diagrams of Figs. 5(a) and 5(b). Note that confocal microscopy measures light in the "mid-field" range, while goniophotometry is a far-field measurement technique. Consequently, goniophotometry measures light emitted from both the chip's top surface and vertical facets, while confocal microscopy mainly detects light from the top surface as most of the light emitted from the facets is beyond the collection cone of the objective (which also depends on the choice of objective). This property is particularly useful for studying the effects of surface texturing (including micro-lenses), screening out light emitted from the facets, which would remain unaltered. Together with high-sensitivity and high-resolution detection, confocal microscopy has been demonstrated as a powerful tool for characterizing LED surface texturing effects.

In summary, an NSL-patterned 1-μm closed-packed lens array has been integrated onto the sapphire surface of an InGaN flip-chip LED. The high-density lens array promotes light extraction without deteriorating electrical performance, as well as reducing emission divergence, making them useful in applications requiring lower divergence beams. 3-D emission patterns of the devices have been imaged directly using confocal microscopy, from which reduced emission divergence can be observed. Additionally, angular emission plots have been extracted from 2-D cross-sectional confocal emission plots, from which emission FWHM angles can be evaluated.
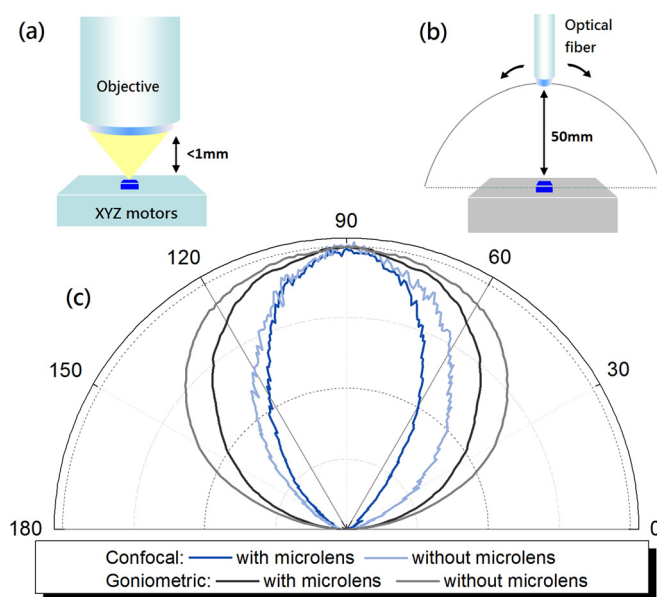
FIG. 5. Schematic diagrams illustrating the experimental setups of (a) confocal microscopy and (b) goniophotometry. (c) Angular emission plots obtained from goniophotometry, as well as plots generated from confocal microscopy data, for the LEDs with and without micro-lenses.

[1] Y. K. Ee, P. Kumnorkaew, R. A. Arif, H. Tong, H. Zhao, J. F. Gilchrist, and N. Tansu, IEEE J. Sel. Top. Quantum Electron. **15**, 1218 (2009).

[2] H. W. Choi, C. Liu, E. Gu, G. McConnell, J. M. Girkin, I. M. Watson, and M. D. Dawson, Appl. Phys. Lett. **84**, 2253 (2004).

[3] M. Khizar, Z. Y. Fan, K. H. Kim, J. Y. Lin, and H. X. Jiang, Appl. Phys. Lett. **86**, 173504 (2005).

[4] J. J. Wierer, D. A. Steigerwald, M. R. Krames, J. J. O'Shea, M. J. Ludowise, G. Christenson, Y. C. Shen, C. Lowery, P. S. Martin, S. Subramanya, W. Goetz, N. F. Gardner, R. S. Kern, and S. A. Stockman, Appl. Phys. Lett. **78**, 3379 (2001).

[5] S. J. Chang, C. S. Chang, Y. K. Su, C. T. Lee, W. S. Chen, C. F. Shen, Y. P. Hsu, S. C. Shei, and H. M. Lo, IEEE Trans. Adv. Packag. **28**, 273 (2005).

[6] S. H. Huang, R. H. Horng, K. S. Wen, Y. F. Lin, K. W. Yen, and D. S. Wuu, IEEE Photon. Technol. Lett. **18**, 2623 (2006).

[7] D. S. Han, J. Y. Kim, S. I. Na, S. H. Kim, K. D. Lee, B. Kim, and S. J. Park, IEEE Photon. Technol. Lett. **18**, 1406 (2006).

[8] W. N. Ng, C. H. Leung, P. T. Lai, and H. W. Choi, Nanotechnology **19**, 255302 (2008).

[9]J. H. Son, J. U. Kim, Y. H. Song, B. J. Kim, C. J. Ryu, and J. L. Lee, Adv. Mater. **24**, 2259 (2012).

[10]J. J. Chen, Y. K. Su, C. L. Lin, S. M. Chen, W. L. Li, and C. C. Kao, IEEE Photon. Technol. Lett. **20**, 1193 (2008).

[11]C. Griffin, E. Gu, H. W. Choi, C. W. Jeon, G. McConnell, J. M. Girkin, and M. D. Dawson, Appl. Phys. Lett. **86**, 041111 (2005).

[12]T. N. Oder, J. Shakya, J. Y. Lin, and H. X. Jiang, Appl. Phys. Lett. **82**, 3692 (2003).

[13]L. Kuna, C. Sommer, E. Zinterl, F. P. Wenzl, P. Pachler, P. Hartmann, S. Tasch, and G. Leising, Appl. Phys. B: Lasers Opt. **91**, 571 (2008).

[14]A. David, T. Fujii, R. Sharma, K. McGroddy, S. Nakamura, S. P. DenBaars, E. L. Hu, C. Weisbuch, and H. Benisty, Appl. Phys. Lett. **88**, 061124 (2006).